NMDA receptors regulate $GABA_A$ receptor lateral mobility and clustering at inhibitory synapses through serine 327 on the γ2 subunit

James Muir[a,b], I. Lorena Arancibia-Carcamo[a,1], Andrew F. MacAskill[a,1], Katharine R. Smith[a,1], Lewis D. Griffin[c], and Josef T. Kittler[a,2]

[a]Department of Neuroscience, Physiology, and Pharmacology, [b]Centre for Mathematics and Physics in the Life Sciences and Experimental Biology, and [c]Department of Computer Science, University College London, London WC1E 6BT, United Kingdom

Edited by Pietro De Camilli, Yale University and Howard Hughes Medical Institute, New Haven, CT, and approved August 10, 2010 (received for review January 15, 2010)

Modification of the number of $GABA_A$ receptors ($GABA_A$Rs) clustered at inhibitory synapses can regulate inhibitory synapse strength with important implications for information processing and nervous system plasticity and pathology. Currently, however, the mechanisms that regulate the number of $GABA_A$Rs at synapses remain poorly understood. By imaging superecliptic pHluorin tagged $GABA_A$R subunits we show that synaptic $GABA_A$R clusters are normally stable, but that increased neuronal activity upon glutamate receptor (GluR) activation results in their rapid and reversible dispersal. This dispersal correlates with increases in the mobility of single $GABA_A$Rs within the clusters as determined using single-particle tracking of $GABA_A$Rs labeled with quantum dots. GluR-dependent dispersal of $GABA_A$R clusters requires Ca^{2+} influx via NMDA receptors (NMDARs) and activation of the phosphatase calcineurin. Moreover, the dispersal of $GABA_A$R clusters and increased mobility of individual $GABA_A$Rs are dependent on serine 327 within the intracellular loop of the $GABA_A$R γ2 subunit. Thus, NMDAR signaling, via calcineurin and a key $GABA_A$R phosphorylation site, controls the stability of synaptic $GABA_A$Rs, with important implications for activity-dependent control of synaptic inhibition and neuronal plasticity.

ion channels | plasticity | trafficking | diffusion | calcineurin

Synaptic inhibition plays a critical role in regulating neuronal excitability and information processing in the brain. The number of $GABA_A$ receptors ($GABA_A$Rs) in the surface membrane and at synaptic sites is an important determinant of inhibitory synapse strength (1), but the mechanisms that rapidly control synaptic $GABA_A$R number and stability remain poorly understood. Activation of Ca^{2+}-permeable ionotropic glutamate receptors (GluRs) during plasticity and in pathology can result in down-modulation of inhibitory synapse strength and $GABA_A$R function (2–5) but the molecular and cellular mechanisms underlying GluR-dependent changes in the strength of GABAergic inhibition remain unclear.

A major mechanism for modulating $GABA_A$R activity is the direct phosphorylation of residues within the intracellular loops of $GABA_A$R subunits, which can regulate synaptic inhibition, $GABA_A$R channel kinetics, and trafficking (6–9). The rapid movement of neurotransmitter receptors (including $GABA_A$Rs) (10–12) into and out of synapses has also recently emerged as an important mechanism for regulating synaptic strength (13). However, whether $GABA_A$R phosphorylation can directly regulate the synaptic stability of $GABA_A$Rs and their lateral diffusion and movement into and out of synapses is unknown.

Here, by live cell imaging of surface $GABA_A$R clusters with pH-sensitive superecliptic pHluorin (SEP) and single $GABA_A$Rs with quantum dots (QDs), we investigate the mechanisms that regulate activity-dependent control of the lateral diffusion, clustering, and stability of $GABA_A$Rs at inhibitory synapses. We find that Ca^{2+} entry through NMDA receptors (NMDARs) leads to a reversible dispersal of $GABA_A$R clusters and an increase in $GABA_A$R lateral mobility. This mechanism can also allow for a localized $GABA_A$R dispersal in dendrites when only a few excitatory synapses are activated. The dispersal of $GABA_A$Rs from synapses requires activation of the phosphatase calcineurin, and is dependent on serine 327, a key phosphorylation site in the $GABA_A$R γ2 subunit (14). Thus, activity-dependent control of phospho-dependent signaling can rapidly regulate the number of synaptic $GABA_A$Rs with important implications for inhibitory synaptic plasticity, pathology, and information processing in the brain.

Results

$GABA_A$R Clusters Are Stable Under Basal Conditions, Although Single $GABA_A$Rs Can Be Highly Mobile. To image surface $GABA_A$R clusters in the dendrites of live cultured hippocampal neurons, we expressed SEP-tagged $GABA_A$R α2 subunits ($\alpha2^{SEP}$-$GABA_A$Rs) (Fig. S1*A*) (15), the majority of which formed bright fluorescent clusters along the neuronal dendrites in addition to lower levels of diffuse staining (Fig. 1*A*). Heterologously expressed α2-SEP subunits could not access the cell surface without the presence of coexpressed $GABA_A$R β- and γ2 subunits (Fig. S1 *B* and *C*) and thus cannot form homomeric surface $GABA_A$Rs. In agreement with this, immunoprecipitating native $GABA_A$Rs from α2-SEP subunit transfected neurons followed by Western blotting with GFP antibodies confirmed that α2-SEP subunits assembled with endogenous $GABA_A$R subunits, and the lack of any cleavage products confirmed that the fluorescence from $\alpha2^{SEP}$-$GABA_A$Rs was reporting only full-length α2-SEP subunits (Fig. S1*D*). $\alpha2^{SEP}$-$GABA_A$R fluorescence was rapidly and reversibly eclipsed by transient exposure to low extracellular pH buffer, which completely eclipsed the signal (Fig. S1 *E–H*), confirming surface expression of the clusters. A large fraction of $\alpha2^{SEP}$-$GABA_A$R clusters (84.3 ± 1.8%) were localized to inhibitory synapses marked by GAD-6 staining (Fig. S1*I*) and 65.3 ± 5.2% were apposed to FM4-64 labeled presynaptic terminals (Fig. S1*J*, in agreement with previous reports for the proportion of native $GABA_A$R clusters found opposite active FM dye-labeled presynaptic terminals) (16, 17). However, only 9.1 ± 1.3% were found apposed to excitatory synapses labeled with homer1 (Fig. S1*K*). Thus, α2-SEP fluorescence reports surface heteromeric $GABA_A$Rs that accumulate in clusters at inhibitory synapses.

Author contributions: J.M., I.L.A.-C., A.F.M., K.R.S., L.D.G., and J.T.K. designed research; J.M., I.L.A.-C., A.F.M., and K.R.S. performed research; I.L.A.-C. contributed new reagents/analytic tools; J.M., I.L.A.-C., and K.R.S. analyzed data; and J.M. and J.T.K. wrote the paper.

The authors declare no conflict of interest.

This article is a PNAS Direct Submission.

[1]I.L.A.-C., A.F.M., and K.R.S. contributed equally to this work.

[2]To whom correspondence should be addressed. E-mail: j.kittler@ucl.ac.uk.

This article contains supporting information online at www.pnas.org/lookup/suppl/doi:10.1073/pnas.1000589107/-/DCSupplemental.

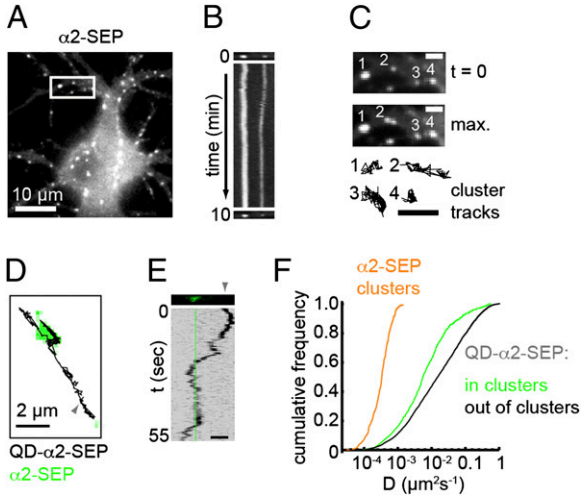

Fig. 1. Surface $GABA_AR$ clustering under basal conditions. (*A*) $\alpha2^{SEP}$-$GABA_ARs$ expressed in cultured hippocampal neurons. (*B*) Kymograph (a line scan vertically projected over time) showing stability of $\alpha2^{SEP}$-$GABA_AR$ clusters in boxed region in *A* over the movie (duration 10 min). (*C*) Region boxed in *A* shown at $t = 0$ (*Top*), as a maximum projection over time (*Middle*) and with cluster trajectories shown (*Bottom*) (3× zoom). (Scale bars, 2 μm.) (*D*) Trajectory of a QD-tagged $\alpha2^{SEP}$-$GABA_AR$ (black, origin marked by gray arrowhead) undergoing lateral diffusion into and out of an $\alpha2^{SEP}$-$GABA_AR$ cluster (green). (*E*) Kymograph for trajectory in *D*. Note the period of low horizontal displacement corresponding to confined motion within cluster (position marked by green line). (Scale bar, 2 μm.) (*F*) $\alpha2^{SEP}$-$GABA_AR$ cluster diffusion coefficients (orange) and instantaneous diffusion coefficients for QD-$\alpha2^{SEP}$-$GABA_ARs$ inside (green) and outside of clusters (black). Single $GABA_ARs$ are less mobile when within $GABA_AR$ clusters [$P = 4 \times 10^{-13}$, Kolmogorov–Smirnov (K-S) test, $n_{in} = 598$, $n_{out} = 3665$].

Under resting conditions, continuous imaging revealed that the intensities and locations of $\alpha2^{SEP}$-$GABA_AR$ clusters were stable for periods of 10 min (Fig. 1 *A–C*) although interestingly, some clusters exhibited small, asynchronous lateral movements (Fig. 1 *B* and *C*). Tracking the mass centers of individual clusters gave trajectories that were used to determine their diffusivities. The low mean diffusivity of $\alpha2^{SEP}$-$GABA_AR$ clusters (6×10^{-4} $\mu m^2 \cdot s^{-1}$, Fig. 1*F* and Movie S1) is similar to that previously reported for clusters of the inhibitory postsynaptic scaffold gephyrin (18), suggesting that $\alpha2^{SEP}$-$GABA_AR$ cluster movement may represent movement of the entire inhibitory postsynaptic apparatus.

Although imaging of $\alpha2^{SEP}$-$GABA_ARs$ allowed the behavior of synaptic $GABA_AR$ clusters to be followed, it could not resolve the behavior of individual $GABA_ARs$. To simultaneously visualize synaptic $GABA_AR$ clusters and single $GABA_ARs$, we combined SEP tagging with QD tracking (13, 19, 20). Single $\alpha2^{SEP}$-$GABA_ARs$ were labeled using a low concentration of GFP antibody to recognize the extracellular SEP tag on the α2 subunit in conjunction with an anti-mouse secondary coupled to 605-nm QDs (Fig. S2*A*). In contrast to the relative immobility of $\alpha2^{SEP}$-$GABA_AR$ clusters, single QD-labeled $\alpha2^{SEP}$-$GABA_ARs$ could be observed to rapidly diffuse into and out of $GABA_AR$ clusters (Fig. 1 *D* and *E* and Movie S2). QD-labeled $\alpha2^{SEP}$-$GABA_ARs$ were less mobile when inside $GABA_AR$ clusters (median $D_{in} = 0.0078$ $\mu m^2 \cdot s^{-1}$, median $D_{out} = 0.0192$ $\mu m^2 \cdot s^{-1}$, Fig. 1*F*) and exhibited confined motion within clusters (Fig. S2 *B* and *C*), presumably due to interactions with the scaffold gephyrin. $\alpha2^{SEP}$-$GABA_AR$ mobility and residency time were similar inside clusters whether or not these were apposed to FM 4-64 positive puncta (Fig. S2 *D–F*). Native $GABA_ARs$ imaged by QD tracking could also be found either confined at inhibitory postsynaptic domains labeled by expression of GFP-tagged gephyrin or seen to rapidly diffuse into and out of these structures (Fig. S2 *G–J*). Thus, while clusters of synaptic $GABA_ARs$ remain stable over time, single receptors can rapidly exchange between synaptic and extrasynaptic locations, providing a potential mechanism for rapid regulation of synaptic $GABA_AR$ number.

Ca^{2+} Influx Through NMDARs Causes Rapid Dispersal of Surface $GABA_AR$ Clusters. To directly examine the influence of neuronal activity on $GABA_AR$ clustering in live neurons we investigated the effect of altering excitatory synaptic activity by activating GluRs. Perfusion of 30 μM glutamate and 1 μM glycine for 4 min caused a rapid dispersal of surface $\alpha2^{SEP}$-$GABA_AR$ clusters (Fig. 2 *A–D* and Movie S3). At $t = 9$ min, $\alpha2^{SEP}$-$GABA_AR$ cluster intensities were significantly decreased [fluorescence in clusters at $t = 9$ min normalized to $t = 0$ (cluster F/F_0); control, 0.95 ± 0.02; glut/gly, 0.65 ± 0.05, $P = 0.0001$]. Loss of clustered $\alpha2^{SEP}$-$GABA_AR$ fluorescence on GluR activation was significantly reduced in zero extracellular Ca^{2+} (cluster F/F_0: 0.87 ± 0.03, $P = 0.005$) or in the presence of the NMDAR antagonist APV (cluster F/F_0: 0.86 ± 0.02, $P = 0.0003$), confirming that synaptic $\alpha2^{SEP}$-$GABA_AR$ cluster dispersal driven by GluR activation was dependent on extracellular Ca^{2+} entry via NMDARs (Fig. 2 *A–C*). Interestingly, $GABA_AR$ activation was not required for GluR-dependent $\alpha2^{SEP}$-$GABA_AR$ cluster dispersal, which was also seen in the presence of the $GABA_AR$ antagonist bicuculline (100 μM) (cluster F/F_0: 0.74 ± 0.04, $P = 0.001$, Fig. 2*C*).

In contrast to the decrease in fluorescence of $\alpha2^{SEP}$-$GABA_AR$ clusters, the total fluorescence in dendrites remained unaltered (Fig. 2*C*, F/F_0, control, 0.96 ± 0.01; glut/gly, 0.92 ± 0.01, $P > 0.05$), suggesting a redistribution of $GABA_ARs$ at the plasma membrane (i.e., out of clusters and into extrasynaptic regions), rather than their removal from the cell surface. Dynamin and AP2-dependent endocytosis can rapidly modify the number of synaptic $GABA_ARs$ (21–23) and occurs predominantly at extrasynaptic sites (24). Pretreatment of neurons with the dynamin inhibitor dynasore (10 min, 80 μM) (25, 26) did not prevent the loss of clustered $\alpha2^{SEP}$-$GABA_AR$ fluorescence (Fig. 2 *E–G*, cluster F/F_0: vehicle, 0.93 ± 0.01; dynasore + glut/gly, 0.69 ± 0.04, $P = 3 \times 10^{-5}$), confirming that the observed loss of $GABA_AR$ clusters is due to cell surface dispersal of $\alpha2^{SEP}$-$GABA_ARs$ and not endocytosis. In agreement with this, $\alpha2^{SEP}$-$GABA_AR$ fluorescence in perisynaptic regions surrounding clusters could be seen to transiently increase on GluR activation (Fig. 2 *H* and *I*), and the variance in the distribution of $\alpha2^{SEP}$-$GABA_AR$ fluorescence intensities in neuronal processes at $t = 9$ min was significantly decreased by GluR activation (normalized to variance at $t = 0$: control, 0.97 ± 0.03; glut/gly, 0.73 ± 0.03, $P = 0.001$, Fig. 2*D*), suggesting a more diffuse $GABA_AR$ distribution (cluster dispersal). The above results were confirmed for native receptors as GluR activation did not change the total intensity of native surface $GABA_ARs$ in dendrites but significantly decreased the variance of pixel intensities in dendrites, suggesting that surface clusters of native $GABA_ARs$ are also dispersed upon GluR activation (Fig. S3). Moreover, surface biotinylation to directly quantify the effect of GluR activation on native $GABA_AR$ levels revealed no change in the surface fraction of the γ2 subunit (glut/gly: 92 ± 6.2% of control, $P > 0.05$, paired *t* test, Fig. 2 *J* and *K*). These data suggest that $GABA_AR$ cluster dispersal upon GluR activation is due to lateral movement of $GABA_ARs$ out of synaptic clusters and into the extrasynaptic plasma membrane.

Activity-Dependent $GABA_AR$ Cluster Dispersal Is Reversible and Can Be Induced by Local, Synaptic Glutamate Release. The activity-induced movement of $GABA_ARs$ out of synapses and into the extrasynaptic space suggests a pool of redistributed surface receptors available for eventual replenishment of synaptic $GABA_AR$ content. To further investigate this possibility we imaged $\alpha2^{SEP}$-$GABA_AR$ cluster fluorescence for longer periods after GluR activation to determine whether $GABA_AR$ clusters could

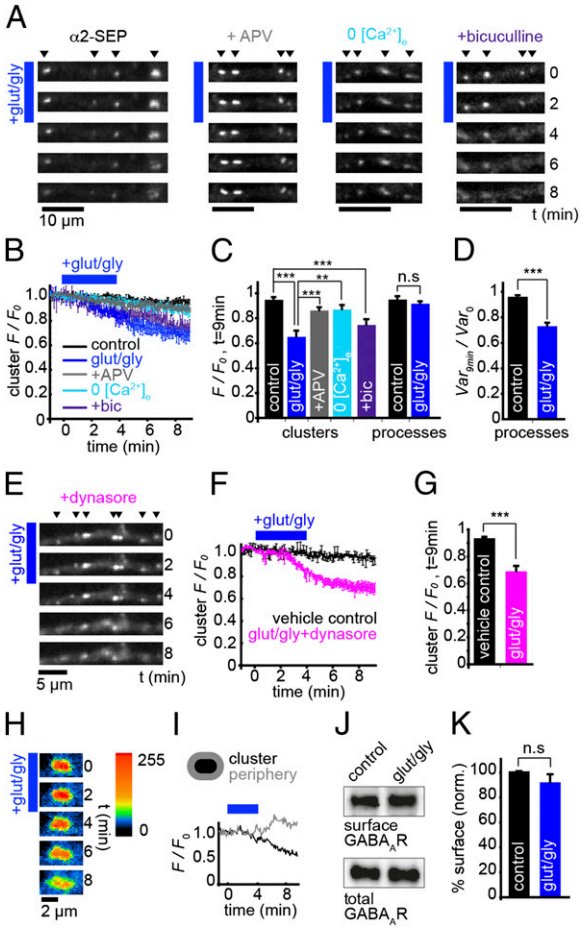

Fig. 2. $GABA_AR$ clusters disperse on GluR activation. (*A*) $\alpha2^{SEP}$-$GABA_AR$ clusters disperse on GluR activation (blue bar), which requires Ca^{2+} influx through NMDA receptors but not $GABA_AR$ activity. (*B*) Time course of $\alpha2^{SEP}$-$GABA_AR$ cluster F/F_0: control, black, $n = 6$ cells; glut/gly, dark blue, $n = 6$; in presence of APV, gray, $n = 8$; in 0 $[Ca^{2+}]_e$, light blue, $n = 5$; in presence of bicuculline, purple, $n = 4$. (*C*) Summary of cluster F/F_0 at $t = 9$ min after initial GluR activation. Loss of fluorescence in $\alpha2^{SEP}$-$GABA_AR$ clusters on GluR activation is significant compared with control ($P = 0.0001$) and is significantly blocked in 0 $[Ca^{2+}]_e$ ($P = 0.005$) and by APV ($P = 0.0003$), but not by bicuculline ($P = 0.001$ compared with control). Overall fluorescence in processes is not altered by GluR activation ($P > 0.05$). (*D*) Variance normalized to $t = 0$ (Var/Var_0) in processes at $t = 9$ min after initial GluR activation. Variance in pixel intensity is decreased significantly by GluR activation ($P = 0.001$). (*E*) $\alpha2^{SEP}$-$GABA_AR$ clusters disperse on GluR activation when endocytosis is blocked. (*F*) Time course of $\alpha2^{SEP}$-$GABA_AR$ cluster F/F_0: vehicle, black, $n = 7$ cells; glut/gly after pretreatment with dynasore, pink, $n = 7$. (*G*) Cluster F/F_0 at $t = 9$ min. Loss of fluorescence in $\alpha2^{SEP}$-$GABA_AR$ clusters is significant compared with vehicle control ($P = 3 \times 10^{-5}$). (*H*) Close-up of $\alpha2^{SEP}$-$GABA_AR$ dispersal on GluR activation (blue bar). Intensity is represented by a custom look-up table. (*I*) F/F_0 in perisynaptic region surrounding cluster (gray) increases as F/F_0 in cluster (black) decreases, indicating receptor dispersal. (*J*) Blot showing surface biotinylated $GABA_AR$ γ2 subunit and total γ2 subunit for control and glut/gly treatment. (*K*) Surface $GABA_AR$-γ2 fraction is unaffected by glut/gly treatment (91.2 ± 6.2%, $P > 0.05$, paired t test, $n = 4$).

recover from dispersal (Fig. 3 *A–C*). $GABA_AR$ clusters were dispersed at $t = 10$ min after initial drug application (cluster F/F_0, control, 1.00 ± 0.01; glut/gly, 0.70 ± 0.03, $P = 0.001$), but 40 min after GluR activation, $\alpha2^{SEP}$-$GABA_AR$ clustering had fully recovered (cluster F/F_0, control, 0.95 ± 0.03; glut/gly, 0.94 ± 0.06, $P > 0.05$, Fig. 3*C*), suggesting a return of $\alpha2^{SEP}$-$GABA_ARs$ back to synapses on longer timescales. Cluster recovery was not due to recycling of receptors that had been internalized upon GluR

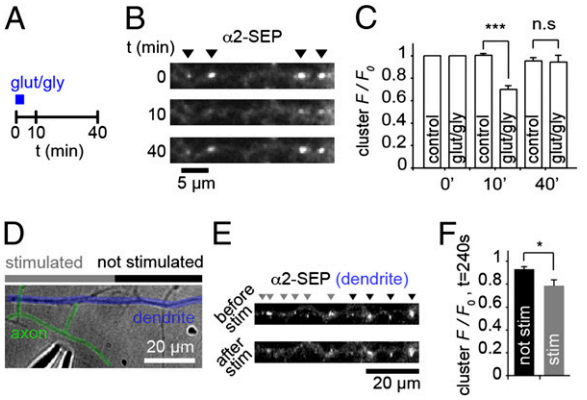

Fig. 3. $GABA_AR$ cluster dispersal is reversible and can be induced by local glutamate release. (*A*) Schematic of recovery experiment. Images were taken at 0, 10, and 40 min. (*B*) $\alpha2^{SEP}$-$GABA_AR$ clustering can recover after dispersal induced by GluR activation. (*C*) Cluster F/F_0 at $t = 0$, 10, and 40 min. Loss of $\alpha2^{SEP}$-$GABA_AR$ cluster fluorescence is significant at $t = 10$ min ($P = 0.001$) but is not significantly different at $t = 40$ min ($P > 0.05$), $n_{control} = 5$ cells, $n_{glut/gly} = 5$ cells. (*D*) DIC image showing local stimulation of axon (colored green) crossing $\alpha2^{SEP}$-$GABA_AR$ containing dendrites (blue), using a glass microelectrode (lower left). (*E*) $\alpha2^{SEP}$-$GABA_AR$ fluorescence on dendrite in *D* before and after electrical stimulus (20 Hz, 1 min). Clusters are marked by gray arrows in stimulated regions (within 15 μm of apparent axonal contacts) and by black arrows in unstimulated regions. (*F*) F/F_0 at $t = 240$ s is significantly reduced in stimulated regions compared with unstimulated regions ($P = 0.014$, $n = 8$ cells).

stimulation, as dynasore treatment did not block the recovery from dispersal (Fig. S4). To explore the possibility that synaptic activation could cause local $GABA_AR$ dispersal, we used a patch pipette to locally stimulate axons crossing dendrites expressing $\alpha2^{SEP}$-$GABA_ARs$ (Fig. 3*D*). By maximally stimulating single axons, we found that fluorescence from clusters in stimulated regions (<15 μm from stimulated synapses) was rapidly decreased (at $t = 240$ s, cluster F/F_0 was 0.94 ± 0.02 in unstimulated regions and 0.79 ± 0.05 in stimulated regions, $P = 0.014$, Fig. 3 *E* and *F*, time course in Fig. S5), dependent on action potential firing and GluR activation (Fig. S5). Thus, $GABA_AR$ dispersal is reversible and can be triggered by glutamate released from single or a few synapses with important implications for plasticity and control of local dendritic excitability.

GluR Activation Increases $GABA_AR$ Lateral Mobility. To further explore GluR-driven modulation of $GABA_AR$ surface movement we examined the dynamics of single QD-tagged $\alpha2^{SEP}$-$GABA_ARs$, which allowed us to directly monitor the behavior of single $GABA_ARs$ with respect to the positions of the synaptically localized $GABA_AR$ clusters. GluR activation resulted in a significant increase in the surface mobility of $GABA_ARs$ both inside and outside of $\alpha2^{SEP}$-$GABA_AR$ clusters [median D_{in} increased 1.87-fold from 0.0078 to 0.0146 $\mu m^2 \cdot s^{-1}$, $P = 8 \times 10^{-8}$; median D_{out} increased 1.16-fold from 0.0192 to 0.0219 $\mu m^2 \cdot s^{-1}$, $P = 4 \times 10^{-10}$, Kolmogorov–Smirnov (K-S) test, Fig. 4 *A–C* and Movie S4]. Although the mobility of both receptor pools increased, the difference in mobilities of single $\alpha2^{SEP}$-$GABA_ARs$ was more striking for receptors within clusters, suggesting that the effect of GluR activation on $GABA_AR$ mobility was strongest for receptors at $GABA_AR$ cluster locations (inhibitory synapses). Furthermore, GluR activation strongly decreased the average time spent by single QD-labeled $GABA_ARs$ at $GABA_AR$ clusters (control, 2.35 ± 0.41 s; glut/gly, 1.30 ± 0.17 s, $P = 0.035$, Fig. 4*D*). Using QD tracking to follow the behavior of single native $GABA_ARs$ labeled with antibodies to either α2 or β2/β3 $GABA_AR$ subunits and 605 nm QDs we found that $GABA_ARs$ were notably more dynamic after GluR activation (Fig. S6). Median diffusivity increased 1.20-fold for the α2 subunit and 1.27-fold for the β3 subunit (both $P < 1 \times 10^{-10}$,

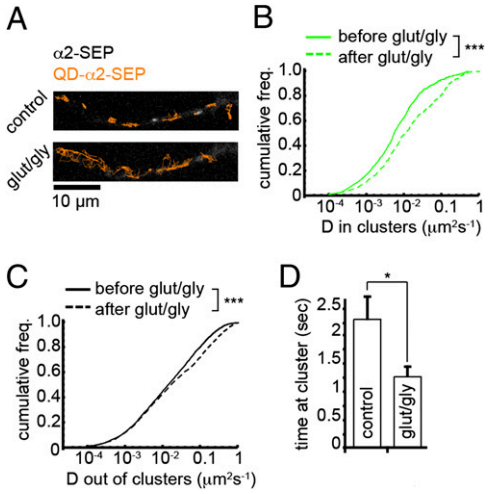

Fig. 4. GluR activation increases $GABA_AR$ lateral mobility and decreases synaptic residency time. (*A*) QD-tagged $\alpha2^{SEP}$-$GABA_AR$ trajectories (orange) before and after GluR activation (t = 9 min) overlaid on $\alpha2^{SEP}$-$GABA_AR$ image. (*B* and *C*) Instantaneous diffusion coefficients for QD-tagged $\alpha2^{SEP}$-$GABA_AR$s before (solid line) and after (dashed line) GluR activation inside (*B*) and outside of clusters (*C*). Mobilities of both pools increased significantly: median D_{in} increased 1.87-fold (n_{before} = 598, n_{after} = 436, $P = 8 \times 10^{-8}$, K-S test); median D_{out} increased 1.16-fold (n_{before} = 3,665, n_{after} = 2,719, $P = 4 \times 10^{-10}$, K-S test). (*D*) Mean residency time of QD-tagged $\alpha2^{SEP}$-$GABA_AR$s at clusters is significantly lower after GluR activation. Control, n = 10 cells; glut/gly, n = 6 cells, P = 0.035.

K-S test). These results describe an effect of GluR activation on individual $GABA_AR$ mobilities consistent with that of $GABA_AR$ dispersal from synaptic clusters.

$GABA_AR$ Cluster Dispersal and Increased Lateral Diffusion Depend on Activation of Calcineurin and Serine 327 in the $GABA_AR$ γ2 Subunit. To investigate the signaling mechanisms involved in NMDAR-mediated $GABA_AR$ cluster dispersal, we asked whether Ca^{2+} influx through NMDARs could activate the phosphatase calcineurin, which has previously been implicated in activity-dependent down-modulation of synaptic inhibition (3, 27). We found that treating cells with a calcineurin autoinhibitory peptide (50 μM, 30 min) or cyclosporin A (20 μM, 10 min, also added in perfusate) did not affect $\alpha2^{SEP}$-$GABA_AR$ cluster intensity (Fig. S7 *A–D*), suggesting that calcineurin has no effect on $GABA_AR$ clustering under basal conditions on this timescale. However, blocking calcineurin activity with the autoinhibitory peptide inhibited $\alpha2^{SEP}$-$GABA_AR$ cluster dispersal on GluR activation [cluster F/F_0, control, 0.92 ± 0.01; glut/gly, 0.71 ± 0.03 ($P = 5 \times 10^{-5}$); treatment, 0.86 ± 0.04, $P = 0.018$ compared with glut/gly, Fig. 5 *A–C*] as did cyclosporin A treatment (Fig. S7 *E–G*). This result suggests that calcineurin activation upon Ca^{2+}influx through NMDARs is directly involved in $GABA_AR$ dispersal.

A major target site for calcineurin-mediated regulation of $GABA_ARs$ is serine 327 (S327) on the γ2 subunit, dephosphorylation of which has been previously shown to lead to a reduction in inhibitory postsynaptic current amplitudes (27). We therefore tested whether S327 is important for NMDAR-mediated $GABA_AR$ cluster dispersal. By Western blotting with a phospho-specific pS327 antibody (27) we found that GluR activation of hippocampal neurons caused a significant decrease in phosphorylation at S327 (normalized to control, pS327/γ2 ratio = 0.55 ± 0.09, $P = 0.035$, paired t test, Fig. 5 *D* and *E*). Using α2-SEP to report $GABA_ARs$ as above, we then cotransfected a myc-tagged γ2 $GABA_AR$ subunit, either with its S327 phosphorylation site intact (γ2-myc) or with S327 mutated to alanine ($\gamma2^{S327A}$-myc). Cotransfection efficiency was found to be ~90% (Fig. S8 *A–C*).

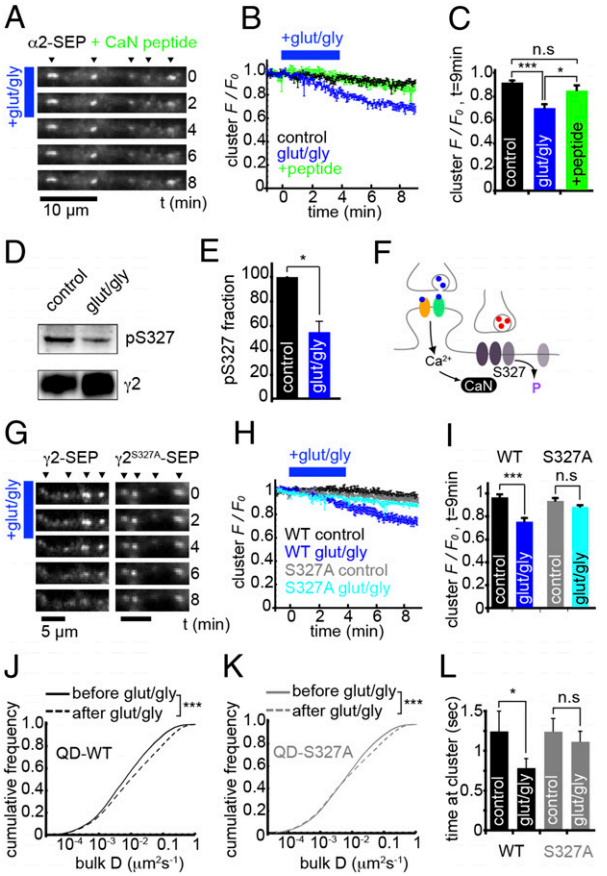

Fig. 5. $GABA_AR$ dispersal is dependent on calcineurin activity and serine 327 in the γ2 subunit. (*A*) $\alpha2^{SEP}$-$GABA_AR$ fluorescence on GluR activation after pretreatment with calcineurin autoinhibitory peptide (CaN peptide). (*B*) Time course of cluster F/F_0; control, black, n = 6 cells; vehicle + glut/gly, blue, n = 5; glut/gly + CaN block, green, n = 6. (*C*) F/F_0 in $\alpha2^{SEP}$-$GABA_AR$ clusters at t = 9 min. $GABA_AR$ dispersal seen under vehicle + glut/gly ($P = 5 \times 10^{-5}$) was blocked by calcineurin inhibitory peptide ($P > 0.05$ vs. control, $P = 0.018$ vs. vehicle + glut/gly). (*D*) Example blot with pS327 and γ2 antibodies from control and glut/gly conditions. Experiments were performed on hippocampal neurons. (*E*) Normalized to control, the ratio of pS327/γ2 decreased to 0.55 ± 0.09 on GluR activation; $P = 0.035$, n = 3. (*F*) Schematic of hypothesized mechanism of GluR-mediated changes in $GABA_AR$ clustering and lateral mobility: dephosphorylation of S327 by calcineurin. (*G*) ^{WT}γ2-SEP and ^{S327A}γ2-SEP fluorescence on GluR activation (blue bar). (*H*) Time course of cluster F/F_0; WT control, black, n = 6 cells; WT glut/gly, blue, n = 8; S327A control, gray, n = 7; S327A glut/gly, light blue, n = 7. (*I*) Cluster F/F_0 at t = 9 min. ^{WT}γ2-SEP clusters disperse on GluR activation ($P = 6 \times 10^{-5}$). However, ^{S327A}γ2-SEP clusters were stable on GluR activation ($P > 0.05$). (*J*) Instantaneous diffusion coefficients for QD-tagged $GABA_ARs$ containing ^{WT}γ2-SEP before (solid line) and after (dashed line) GluR activation. Median D increased 1.43-fold ($P = 2 \times 10^{-16}$, n_{before} = 8,085, n_{after} = 6,316, K-S test). (*K*) As in *J*, for QD-tagged $^{S327A}\gamma2^{SEP}$-$GABA_ARs$. Median D increased 1.06-fold ($P = 2 \times 10^{-16}$, n_{before} = 8,868, n_{after} = 7,327, K-S test). (*L*) Mean residency time of $^{WT}\gamma2^{SEP}$-$GABA_ARs$ at clusters is significantly lower after GluR activation (n = 7 cells, P = 0.04), but not significantly different for $^{S327A}\gamma2^{SEP}$-$GABA_ARs$ (n = 7 cells, $P > 0.05$).

Neurons cotransfected with γ2-myc exhibited robust $\alpha2^{SEP}$-$GABA_AR$ dispersal on GluR activation, but coexpression of $\gamma2^{S327A}$-myc subunits partially blocked cluster dispersal (Fig. S8 *D–H*). Incomplete blockade of cluster dispersal was likely due to α2-SEP subunits being able to assemble with the pool of endogenous γ2 subunits (with their S327 sites intact); therefore, to directly test the influence of S327 on $GABA_AR$ dispersal we imaged $GABA_AR$ clusters with wild-type or mutant SEP-tagged γ2 subunits. S327A mutation did not affect the efficient targeting of $^{S327A}\gamma2^{SEP}$-$GABA_ARs$ to synapses, cluster intensity, or cluster mobility com-

pared with wild type (Fig. S9). However, whereas $GABA_AR$ clusters containing $^{WT}\gamma2$-SEP subunits were dispersed by GluR activation (cluster F/F_0, control, 0.96 ± 0.03; glut/gly, 0.74 ± 0.03, $P = 6 \times 10^{-5}$), $GABA_AR$ clusters containing $^{S327A}\gamma2$-SEP subunits remained stable upon GluR activation (cluster F/F_0, control, 0.93 ± 0.02; glut/gly, 0.88 ± 0.02, $P > 0.05$) (Fig. 5 *G–I*).

We then examined the role of S327 in the γ2 subunit on $GABA_AR$ diffusion dynamics in response to increased neuronal activity. By labeling γ2-SEP subunits with quantum dots via a GFP antibody, we were able to track single $GABA_ARs$ containing either $^{WT}\gamma2$-SEP or $^{S327A}\gamma2$-SEP subunits. Under control conditions, $GABA_ARs$ containing $^{S327A}\gamma2$-SEP subunits were marginally more mobile than $^{WT}\gamma2$-SEP containing receptors (median $D_{WT} = 0.0161\ \mu m^2 \cdot s^{-1}$, median $D_{S327A} = 0.0187\ \mu m^2 \cdot s^{-1}$). On GluR activation, mobilities of $^{WT}\gamma2^{SEP}$-$GABA_ARs$ were much more increased compared with their $^{S327A}\gamma2^{SEP}$-$GABA_AR$ mutant counterparts (Fig. 5 *J* and *K*; median D_{S327A} increased only 1.06-fold from 0.0187 to 0.0199 $\mu m^2 \cdot s^{-1}$, compared with median D_{WT} that increased 1.43-fold from 0.0161 to 0.0231 $\mu m^2 \cdot s^{-1}$, $P = 2 \times 10^{-16}$, K-S test), suggesting that S327A mutation blocked an activity-induced increase in $GABA_AR$ lateral diffusion. Similarly, the residency time of single $^{WT}\gamma2^{SEP}$-$GABA_ARs$ at clusters was significantly decreased by GluR activation (control, 2.29 ± 0.41 s; glut/gly, 1.55 ± 0.20 s, $P = 0.04$), whereas no significant change was seen for $^{S327A}\gamma2^{SEP}$-$GABA_ARs$ (control, 2.16 ± 0.51 s; glut/gly, 2.19 ± 0.36 s, $P > 0.05$) (Fig. 5*L*). Together with the results above, this finding suggests that calcineurin-dependent dephosphorylation of S327 on the γ2 subunit controls activity-dependent changes in the lateral diffusion and clustering of surface $GABA_ARs$.

Discussion

We have investigated the surface behavior of single $GABA_ARs$ and $GABA_AR$ clusters under resting conditions and during increased neuronal activity. Our work provides several important insights into the molecular mechanisms that underlie activity dependence of $GABA_AR$ lateral diffusion and clustering. We show that synaptic $GABA_AR$ clusters are stable under resting conditions whereas single $GABA_ARs$ can be highly mobile. NMDAR activation can cause a rapid increase in surface $GABA_AR$ mobility and a reversible and local dispersal of synaptic $GABA_ARs$ into the extrasynaptic membrane. This mechanism for fast modulation of surface $GABA_AR$ mobility depends on the activity of the phosphatase calcineurin and S327 within the intracellular loop of the γ2 subunit. Our results suggest a cellular mechanism through which GluR signaling can regulate synaptic $GABA_AR$ accumulation on rapid timescales.

Imaging endogenous QD-labeled $GABA_ARs$ does not allow simultaneous visualization of receptor clusters at synapses, and direct imaging of $GABA_AR$ clusters and single receptors has not yet been reported. Simultaneously visualizing $\alpha2^{SEP}$-$GABA_AR$ clusters via SEP fluorescence and single $\alpha2^{SEP}$-$GABA_ARs$ labeled with QDs allowed us to image the behavior of individual receptors compared with synaptic $GABA_AR$ clusters. Using this approach we found that single $\alpha2^{SEP}$-$GABA_ARs$ can be highly dynamic, both inside and outside clusters, and can also rapidly exchange into and out of synaptic $GABA_AR$ clusters. Similar results were also obtained imaging $GABA_ARs$ via a SEP-tagged γ2 subunit. The dynamic nature of single SEP-tagged $GABA_ARs$ was similar to that of endogenous QD-labeled $GABA_ARs$. These observations are in agreement with other recent reports showing that $GABA_ARs$ can be highly dynamic in the plasma membrane (12, 28) and are in line with previous observations of bulk exchange of receptors between synaptic and extrasynaptic locations determined using electrophysiological tagging or fluorescence recovery after photobleaching approaches (10, 11). In contrast to single receptors, $GABA_AR$ clusters were stable for prolonged periods under basal conditions. We did, however, observe small asynchronous oscillatory movements of entire receptor clusters, but these movements were ≈50-fold slower than those of single receptors. The small oscillatory movements of $\alpha2^{SEP}$-$GABA_AR$ clusters are similar to those previously reported for the inhibitory scaffold gephyrin (18), suggesting that the entire inhibitory postsynaptic apparatus (receptor and scaffold) may move together. This observation fits well with the recent observation that $GABA_AR$ α2 subunits interact directly with gephyrin (15) and suggests a tight coupling of the receptor aggregate and scaffold in live cells.

Live cell imaging of SEP-$GABA_AR$ clusters allowed us to directly visualize in real time the role played by neuronal activity in regulating the stability of synaptic $GABA_AR$ clusters. Ca^{2+} entry through NMDARs caused a rapid dispersal of $GABA_AR$ clusters without affecting total surface receptor fluorescence, suggesting that dispersal was due to a redistribution of $GABA_ARs$ out of clusters and into the extrasynaptic membrane. In agreement with this, blocking $GABA_AR$ endocytosis, which is dynamin dependent (21), with the dynamin inhibitor dynasore did not block $GABA_AR$ cluster dispersal. GluR-dependent dispersal of native synaptic $GABA_ARs$ without surface down-modulation was also observed. Moreover, GluR-dependent cluster dispersal correlated with an increase in the lateral mobility of endogenous $GABA_ARs$ and both $\alpha2^{SEP}$-$GABA_ARs$ and $\gamma2^{SEP}$-$GABA_ARs$ as determined using QD tracking. Our results are in line with other recent observations demonstrating that increased neuronal activity generated with the potassium channel blocker 4-AP also leads to an increase in $GABA_AR$ mobilities in dendrites (28).

Dependent on the levels of postsynaptic Ca^{2+}influx, GluR activation can cause either an increase or a decrease in the number or activity of synaptic $GABA_ARs$, via activation of Ca^{2+}-dependent kinases or phosphatases, respectively (2, 27–29). Calcineurin is known to dephosphorylate $GABA_ARs$ on influx of Ca^{2+} through NMDARs (27). In support of a key role for calcineurin in regulating synaptic inhibition via $GABA_AR$ trafficking, we found that this phosphatase underlies the NMDAR-mediated dispersal of $GABA_ARs$ from inhibitory synaptic clusters. Interestingly, calcineurin activity was found to have little influence on the stability or intensity of $GABA_AR$ clusters under resting conditions, in agreement with reports suggesting calcineurin is recruited to $GABA_ARs$ only on increased neuronal activity (27).

Whether changes in $GABA_AR$ phosphorylation state could influence $GABA_AR$ lateral mobility was unknown. Importantly, we found that activity-dependent $GABA_AR$ cluster dispersal and increased lateral mobility were dependent on a well-established $GABA_AR$ phosphorylation site and known target for calcineurin-mediated dephosphorylation (27). GluR activation reduced the phosphorylation of the native γ2 subunit at S327, and mutation of S327 to alanine (S327A) blocked GluR-dependent $GABA_AR$ cluster dispersal. Moreover, by QD tracking $GABA_ARs$ containing mutant γ2 subunits, we found that S327 directly controlled the GluR-dependent increase in $GABA_AR$ lateral mobility and parallel decrease in $GABA_AR$ residency time at synaptic clusters. These results suggest the possibility of an active release mechanism of $GABA_ARs$ from synapses due to S327 dephosphorylation. An interesting topic for future study will be to determine if there is also an activity dependence to $GABA_AR$ lateral mobility in receptors containing nonsynaptic subunit combinations that contribute to tonic conductances (e.g., α5- or δ-containing $GABA_ARs$).

NMDAR-dependent synaptic $GABA_AR$ cluster dispersal has important implications for information processing and is likely to underlie the long-term depression of inhibitory synaptic strength reported to occur during long-term potentiation at excitatory synapses (3, 27). Importantly, imaging SEP-$GABA_ARs$ for longer periods following the activation of GluRs revealed that NMDAR-mediated $GABA_AR$ dispersal is reversible because recovery of cluster fluorescence could be observed on longer (40 min) timescales. Return of receptors on this timescale fits well with the idea that whereas transient $GABA_AR$ dispersal leading to reduced inhibition would favor long-term potentiation at excitatory synapses

and coupling of increased excitability to increased action potential firing (E-S coupling) (3), an eventual "homeostatic" return of $GABA_A$Rs back to synapses would prevent a decrease in synaptic inhibition that may lead to runaway excitation and the generation of seizures. We also demonstrate that $GABA_A$R dispersal can act locally when only a few glutamatergic synapses are activated. Thus synaptic $GABA_A$R cluster dispersal could act to locally enhance dendritic branch excitability and facilitate interactions between neighboring excitatory synapses, with important implications for clustered plasticity and information storage in dendrites (30, 31).

Our findings are also likely to be relevant to neurological disease where prolonged pathological glutamate release, as occurs in epilepsy or stroke, could cause a more sustained shift of $GABA_A$Rs out of synapses and sustained dispersal. This would lead to disinhibition and facilitation of runaway excitation, contributing to neuronal excitotoxicity and disrupted information processing (32, 33). Indeed, NMDAR-mediated dispersal of $GABA_A$Rs out of synapses and into extrasynaptic locations may be the first step that occurs before the activity-dependent down-modulation of surface $GABA_A$Rs that leads to the generation of self-sustaining seizures in status epilepticus (5, 34). Thus, targeting calcineurin and S327-mediated synaptic $GABA_A$R dispersal could also provide a unique therapeutic target for pathological disinhibition in diseases such as epilepsy.

Materials and Methods

Constructs. The N-terminally tagged α2-SEP DNA was a kind gift from S. Moss (Tufts University, Cambridge, MA) and has been described previously (15). For details of construction of mutants, see *SI Materials and Methods*.

Biochemistry. See *SI Materials and Methods*.

Cell Culture and Transfections. Rat hippocampal neurons were prepared and cultured from embryonic day 18 rat brains. Cells were transfected by Amaxa nucleofection as previously described (35). See *SI Materials and Methods*.

Live Cell Imaging. Imaging media used for all experiments contained 125 mM NaCl, 5 mM KCl, 1 mM $MgCl_2$, 2 mM $CaCl_2$, 10 mM D-glucose, and 10 mM Hepes and was adjusted to pH 7.4 with NaOH before use. Cells were imaged under perfusion (4 mL/min) and heating (35–37 °C). See *SI Materials and Methods*.

Fixed Cell Imaging. See *SI Materials and Methods*.

Image Analysis. Images were analyzed in ImageJ. QD tracking was performed using detection and tracking algorithms written in Mathematica (Wolfram Research). See *SI Materials and Methods*.

Local Stimulation. Local electrical stimulation of axons was made using a stimulating electrode via a patch pipette (resistance ~1 MΩ) filled with imaging media (36). See *SI Materials and Methods*.

Statistical Analysis. All experiments were performed on neurons from at least three individual preparations. Unless otherwise stated, *P* values given are from two-tailed *t* tests (type 2) and values are given as mean ± SEM. Error bars represent SEM.

ACKNOWLEDGMENTS. This work was supported by the United Kingdom Medical Research Council (J.T.K.). J.M. is in the Centre for Mathematics and Physics in the Life Sciences and Experimental Biology Ph.D. Program at University College London.

1. Arancibia-Cárcamo IL, Kittler JT (2009) Regulation of GABA(A) receptor membrane trafficking and synaptic localization. *Pharmacol Ther* 123:17–31.
2. Stelzer A, Slater NT, ten Bruggencate G (1987) Activation of NMDA receptors blocks GABAergic inhibition in an in vitro model of epilepsy. *Nature* 326:698–701.
3. Lu YM, Mansuy IM, Kandel ER, Roder J (2000) Calcineurin-mediated LTD of GABAergic inhibition underlies the increased excitability of CA1 neurons associated with LTP. *Neuron* 26:197–205.
4. Gaiarsa JL, Caillard O, Ben-Ari Y (2002) Long-term plasticity at GABAergic and glycinergic synapses: Mechanisms and functional significance. *Trends Neurosci* 25: 564–570.
5. Naylor DE, Liu H, Wasterlain CG (2005) Trafficking of GABA(A) receptors, loss of inhibition, and a mechanism for pharmacoresistance in status epilepticus. *J Neurosci* 25:7724–7733.
6. Kittler JT, Moss SJ (2003) Modulation of GABAA receptor activity by phosphorylation and receptor trafficking: Implications for the efficacy of synaptic inhibition. *Curr Opin Neurobiol* 13:341–347.
7. Vithlani M, Moss SJ (2009) The role of GABAAR phosphorylation in the construction of inhibitory synapses and the efficacy of neuronal inhibition. *Biochem Soc Trans* 37: 1355–1358.
8. Tretter V, et al. (2009) Deficits in spatial memory correlate with modified γ-aminobutyric acid type A receptor tyrosine phosphorylation in the hippocampus. *Proc Natl Acad Sci USA* 106:20039–20044.
9. Wang Q, et al. (2003) Control of synaptic strength, a novel function of Akt. *Neuron* 38:915–928.
10. Thomas P, Mortensen M, Hosie AM, Smart TG (2005) Dynamic mobility of functional GABAA receptors at inhibitory synapses. *Nat Neurosci* 8:889–897.
11. Jacob TC, et al. (2005) Gephyrin regulates the cell surface dynamics of synaptic GABAA receptors. *J Neurosci* 25:10469–10478.
12. Lévi S, et al. (2008) Homeostatic regulation of synaptic GlyR numbers driven by lateral diffusion. *Neuron* 59:261–273.
13. Triller A, Choquet D (2008) New concepts in synaptic biology derived from single-molecule imaging. *Neuron* 59:359–374.
14. Moss SJ, Doherty CA, Huganir RL (1992) Identification of the cAMP-dependent protein kinase and protein kinase C phosphorylation sites within the major intracellular domains of the beta 1, gamma 2S, and gamma 2L subunits of the gamma-aminobutyric acid type A receptor. *J Biol Chem* 267:14470–14476.
15. Tretter V, et al. (2008) The clustering of GABA(A) receptor subtypes at inhibitory synapses is facilitated via the direct binding of receptor alpha 2 subunits to gephyrin. *J Neurosci* 28:1356–1365.
16. Kannenberg K, Sieghart W, Reuter H (1999) Clusters of GABAA receptors on cultured hippocampal cells correlate only partially with functional synapses. *Eur J Neurosci* 11: 1256–1264.
17. Arancibia-Cárcamo IL, et al. (2009) Ubiquitin-dependent lysosomal targeting of GABA (A) receptors regulates neuronal inhibition. *Proc Natl Acad Sci USA* 106:17552–17557.
18. Hanus C, Ehrensperger MV, Triller A (2006) Activity-dependent movements of postsynaptic scaffolds at inhibitory synapses. *J Neurosci* 26:4586–4595.
19. Dahan M, et al. (2003) Diffusion dynamics of glycine receptors revealed by single-quantum dot tracking. *Science* 302:442–445.
20. Groc L, et al. (2004) Differential activity-dependent regulation of the lateral mobilities of AMPA and NMDA receptors. *Nat Neurosci* 7:695–696.
21. Kittler JT, et al. (2000) Constitutive endocytosis of GABAA receptors by an association with the adaptin AP2 complex modulates inhibitory synaptic currents in hippocampal neurons. *J Neurosci* 20:7972–7977.
22. Kittler JT, et al. (2005) Phospho-dependent binding of the clathrin AP2 adaptor complex to GABAA receptors regulates the efficacy of inhibitory synaptic transmission. *Proc Natl Acad Sci USA* 102:14871–14876.
23. Kittler JT, et al. (2008) Regulation of synaptic inhibition by phospho-dependent binding of the AP2 complex to a YECL motif in the GABAA receptor gamma2 subunit. *Proc Natl Acad Sci USA* 105:3616–3621.
24. Bogdanov Y, et al. (2006) Synaptic GABAA receptors are directly recruited from their extrasynaptic counterparts. *EMBO J* 25:4381–4389.
25. Macia E, et al. (2006) Dynasore, a cell-permeable inhibitor of dynamin. *Dev Cell* 10: 839–850.
26. Newton AJ, Kirchhausen T, Murthy VN (2006) Inhibition of dynamin completely blocks compensatory synaptic vesicle endocytosis. *Proc Natl Acad Sci USA* 103:17955–17960.
27. Wang J, et al. (2003) Interaction of calcineurin and type-A GABA receptor gamma 2 subunits produces long-term depression at CA1 inhibitory synapses. *J Neurosci* 23: 826–836.
28. Bannai H, et al. (2009) Activity-dependent tuning of inhibitory neurotransmission based on GABAAR diffusion dynamics. *Neuron* 62:670–682.
29. Marsden KC, Beattie JB, Friedenthal J, Carroll RC (2007) NMDA receptor activation potentiates inhibitory transmission through GABA receptor-associated protein-dependent exocytosis of GABA(A) receptors. *J Neurosci* 27:14326–14337.
30. Harvey CD, Svoboda K (2007) Locally dynamic synaptic learning rules in pyramidal neuron dendrites. *Nature* 450:1195–1200.
31. Losonczy A, Makara JK, Magee JC (2008) Compartmentalized dendritic plasticity and input feature storage in neurons. *Nature* 452:436–441.
32. McNamara JO, Huang YZ, Leonard AS (2006) Molecular signaling mechanisms underlying epileptogenesis. *Sci STKE* 2006:re12.
33. Vogels TP, Abbott LF (2009) Gating multiple signals through detailed balance of excitation and inhibition in spiking networks. *Nat Neurosci* 12:483–491.
34. Goodkin HP, Joshi S, Mtchedlishvili Z, Brar J, Kapur J (2008) Subunit-specific trafficking of GABA(A) receptors during status epilepticus. *J Neurosci* 28:2527–2538.
35. Twelvetrees AE, et al. (2010) Delivery of $GABA_A$Rs to synapses is mediated by HAP1-KIF5 and disrupted by mutant huntingtin. *Neuron* 65:53–65.
36. Macaskill AF, et al. (2009) Miro1 is a calcium sensor for glutamate receptor-dependent localization of mitochondria at synapses. *Neuron* 61:541–555.